Supplement of Atmos. Chem. Phys., 26, 13505–13529, 2026
https://doi.org/10.5194/acp-26-13505-2026-supplement


Atmospheric Chemistry and Physics
Open Access
EGU

*Supplement of*

# Assessment of aerosol iron (Fe) solubility using global dataset – Part 1: Mechanisms underlying the inverse relationship between Fe solubility and Fe concentration

**Kohei Sakata et al.**

*Correspondence to:* Kohei Sakata (kohei.sakata.33@mail.dendai.ac.jp)

**Supporting Text**

**S1. Sampling method for size-fractionated aerosol particles.**

This study provides unpublished total and dissolved Fe and Al concentrations in size-fractionated marine aerosol particles collected in the Pacific Ocean. Size-fractionated aerosol particles were collected during the research cruise of R/V Hakuho-Maru (KH-14-6). A high-volume air sampler (Model-123SL, Kimoto, Japan) was installed on the compass deck at 13 m above sea level. Aerosol samples were separated into seven-size fractions using a Sierra-type cascade impactor (TE-236, Tisch Environmental Inc., USA, Table S1). The aerodynamic diameter ranges for stages 1–7 were >10.2 μm, 4.2–10.2 μm, 2.1–4.2 μm, 1.3–2.1 μm, 0.69–1.3 μm, 0.39–0.69 μm, and <0.39 μm, respectively. In this study, particles larger than 2.1 μm were classified as coarse aerosol particles, whereas those 2.1 μm and smaller were classified as fine aerosol particles. Aerosol particles in stages 1 to 6 were collected on the custom-made polytetrafluoroethylene filter (Sakata et al., 2018, NAFLON™ PTFE tape, Nichias Co., Ltd., Japan). The filter was rinsed following sequential procedures: ultrapure water, 3 mol/L of $HNO_3$, 3 mol/L of HCl, and ultrapure water. The $HNO_3$ and HCl were diluted from concentrated acids with electric grade (Kanto Chemical Co. Inc., Japan). The filter was heated at 150°C for one day in all procedures. The finest fraction was collected on a cellulose filter (Whatman 41, 516 $cm^2$, GE Healthcare, USA), which was not pre-washed before sampling. The proportions of filter blank concentration relative to measurement concentration (=blank + sample) of T-Fe and T-Al were 9.1±4.9% and 2.6±2.7%, respectively.

The total digestion and water extraction of Fe and Al were performed based on Sakata et al. (2022). Briefly, total digestion and water extraction were performed using digested by a mixed acid (2 mL of 15.2 mol $L^{-1}$ $HNO_3$, 2 mL of 9.3 mol $L^{-1}$ HCl, and 1 mL of 20 mol $L^{-1}$ HF, TAMAPURE-AA100). The mixed acid was evaporated to dryness, then the residue was redissolved in 5 mL of 0.15 mol $L^{-1}$ $HNO_3$) and heated at 150°C for a few hours. The solution was filtrated by a hydrophilic PTFE membrane filter (ϕ: 0.20 μm, Dismic®, 25HP020AN, Advantec, Japan). Dissolvable Fe and Al were extracted by 5 mL of ultrapure water with ultrasonication for 30 min. The water-extracted solution was filtrated through the hydrophilic PTFE membrane filter, then the solution was acidified to 0.15 mol $L^{-1}$ of $HNO_3$ by 15.2 mol $L^{-1}$ of $HNO_3$. All sample treatments were performed in a clean booth with HEPA filtrated air condition (SS-MAC 15) installed in a clean room (Class-10000). Total and dissolvable concentrations of Fe and Al were determined by inductively coupled plasma mass spectrometry (ICP-MS, Agilent7700, Agilent, Japan). Iron and Al concentrations were determined by helium gas and non-gas collision modes, respectively.

**Supplemental Figure**

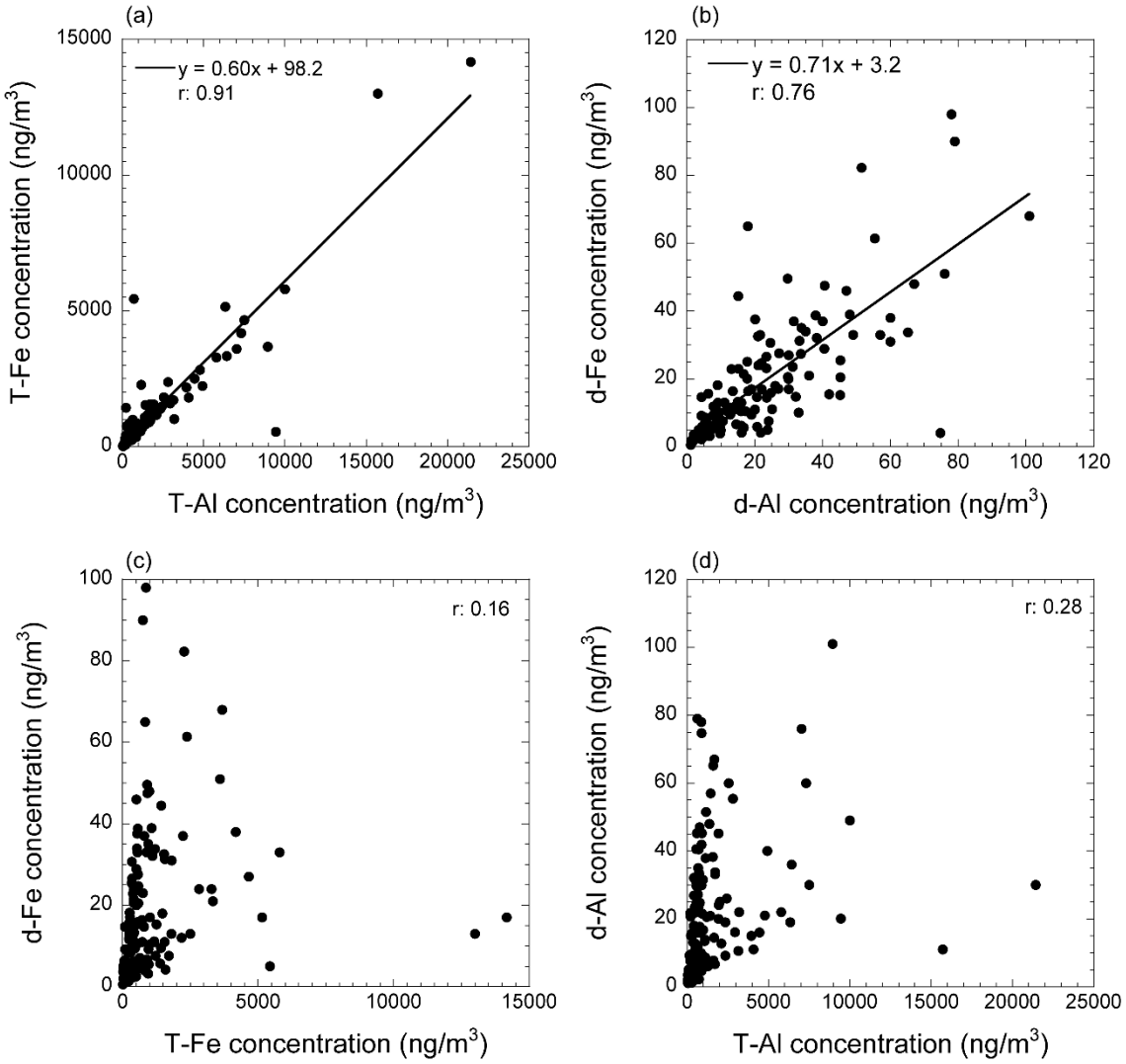


**Figure S1.** Scatter plots (a) between T-Al and T-Fe concentrations, (b) between d-Al and d-Fe concentrations, (c) between T-Fe and d-Fe concentrations, and (d) between T-Al and d-Al concentrations in aerosol particles collected in East Asia.

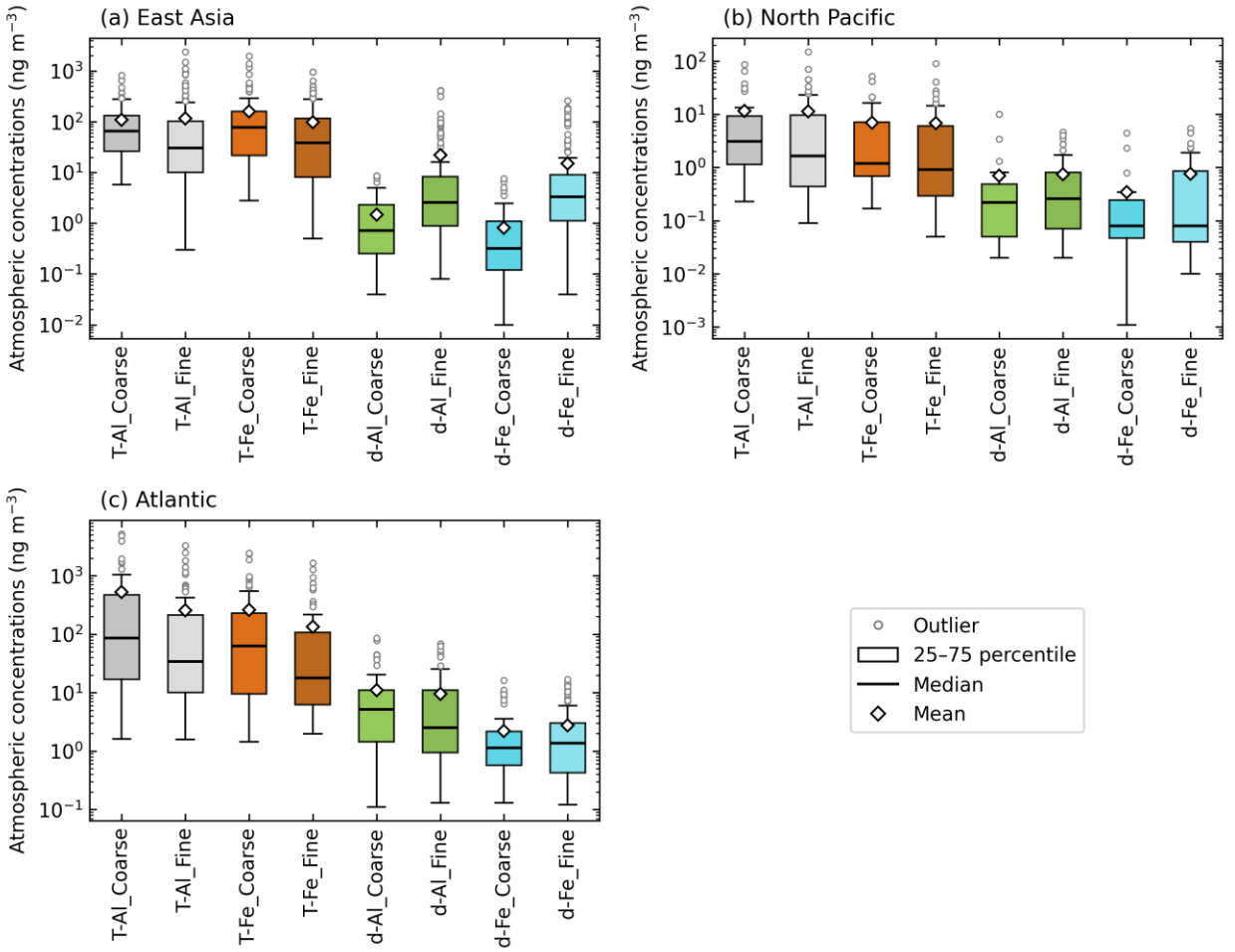


**Figure S2.** Atmospheric concentrations of T-Al, T-Fe, d-Al, and d-Fe in coarse and fine aerosol particles over (a) East Asia, (b) the North Pacific, and (c) the Atlantic.

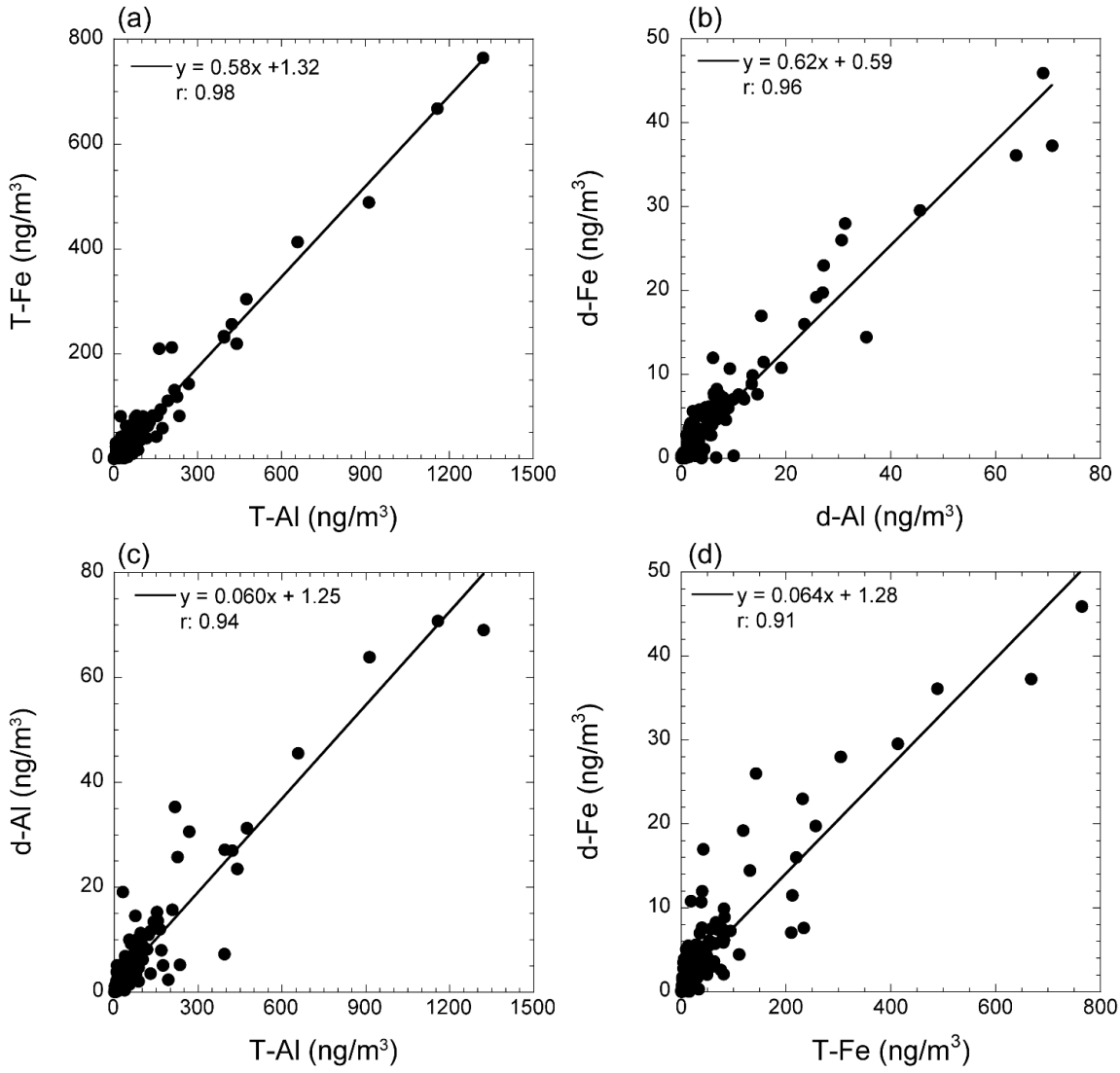


**Figure S3.** Scatter plots (a) between T-Al and T-Fe concentrations, (b) between d-Al and d-Fe concentrations, (c) between T-Fe and d-Fe concentrations, and (d) between T-Al and d-Al concentrations in aerosol particles collected in the North Pacific.

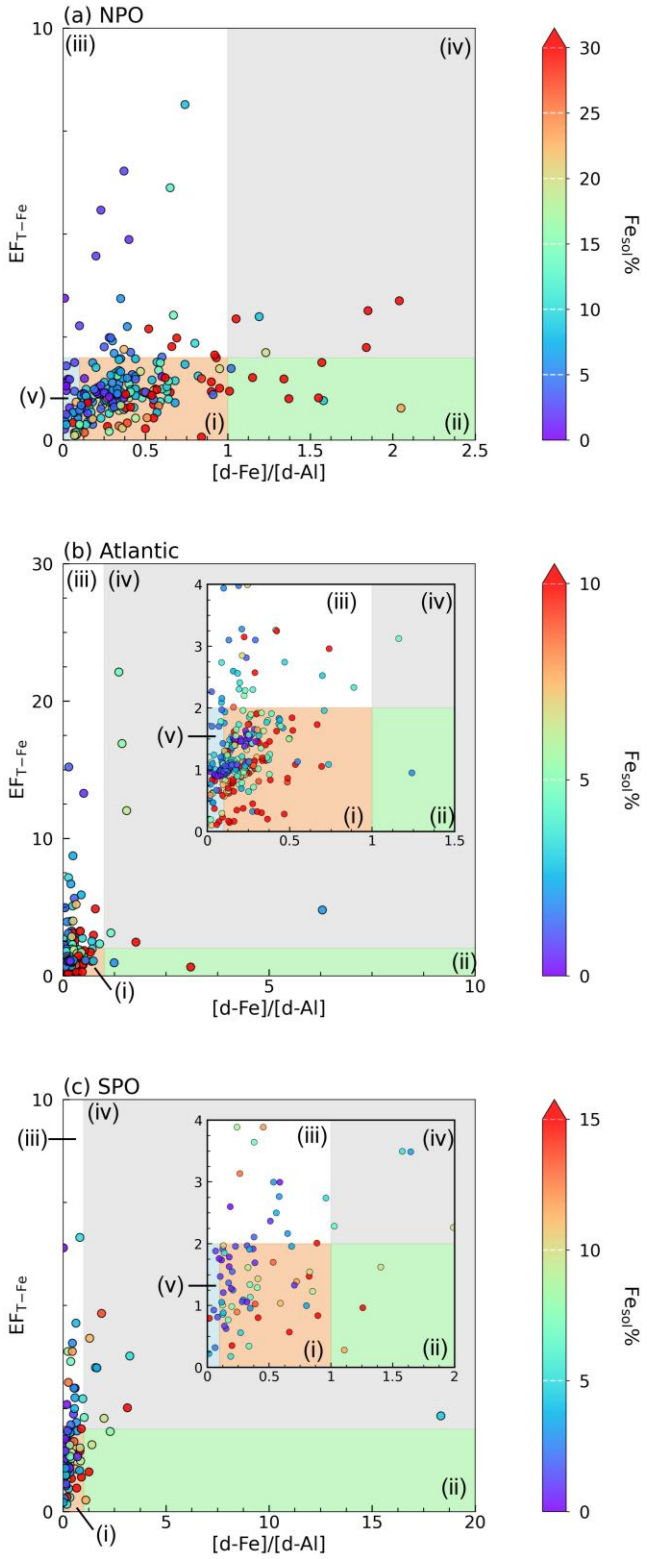


- **Figure S4.** Diagrams between [d-Fe]/[d-Al] ratio and $EF_{T\text{-}Fe}$ in TSP collected above (a) the North Pacific, (b) the Atlantic, and (c) the South Pacific Oceans. Areas (i)–(v) indicate different Fe sources and dissolution processes: (i) proton-promoted dissolution of mineral dust, (ii) ligand-promoted dissolution of mineral dust, (iii) insoluble anthro-Fe, (iv) highly soluble anthro-Fe, and (v) aluminosilicate glass derived from sources such as coal fly ash.

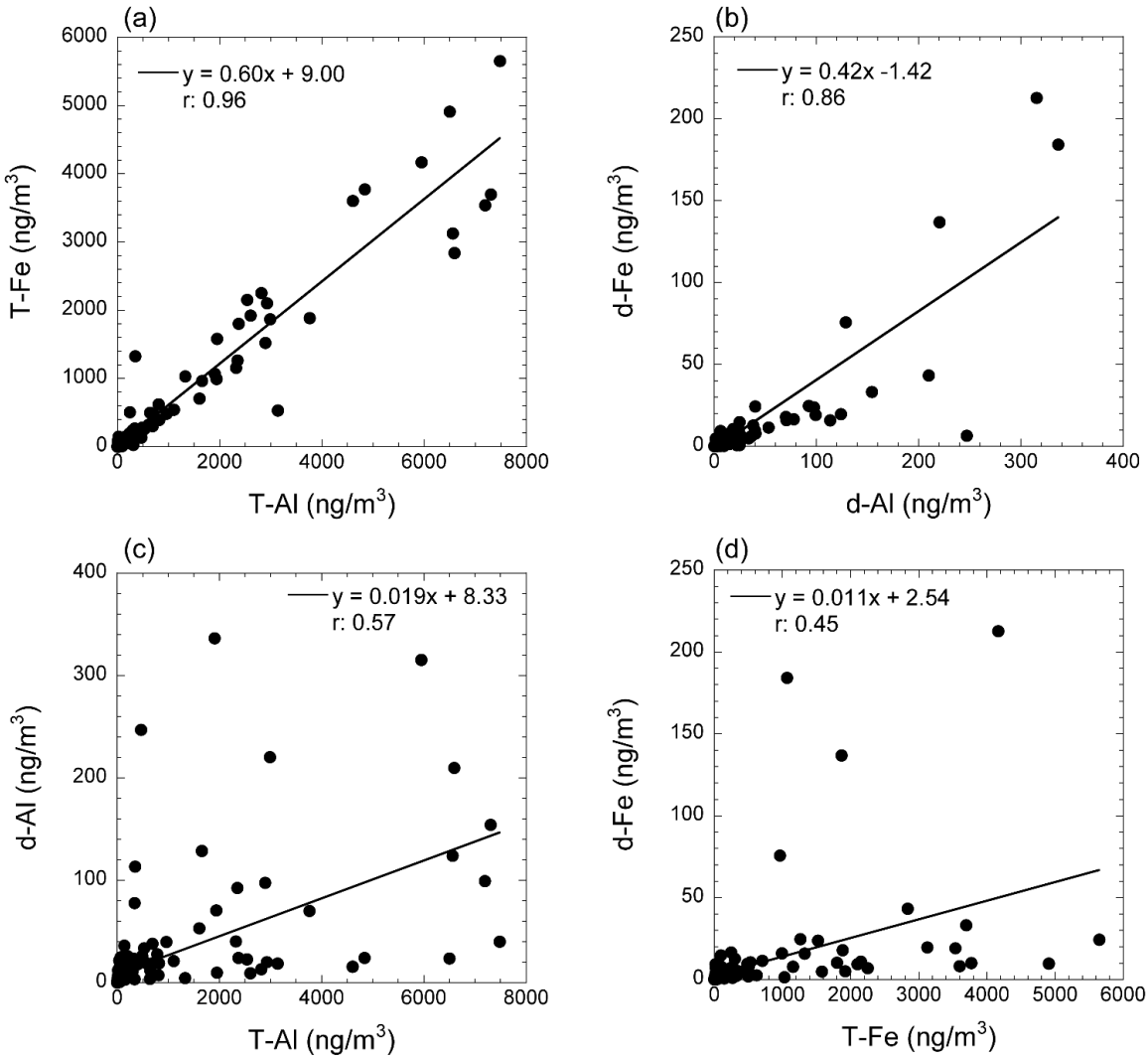


**Figure S5.** Scatter plots (a) between T-Al and T-Fe concentrations, (b) between d-Al and d-Fe concentrations, (c) between T-Fe and d-Fe concentrations, and (d) between T-Al and d-Al concentrations in aerosol particles collected in the Atlantic Ocean.

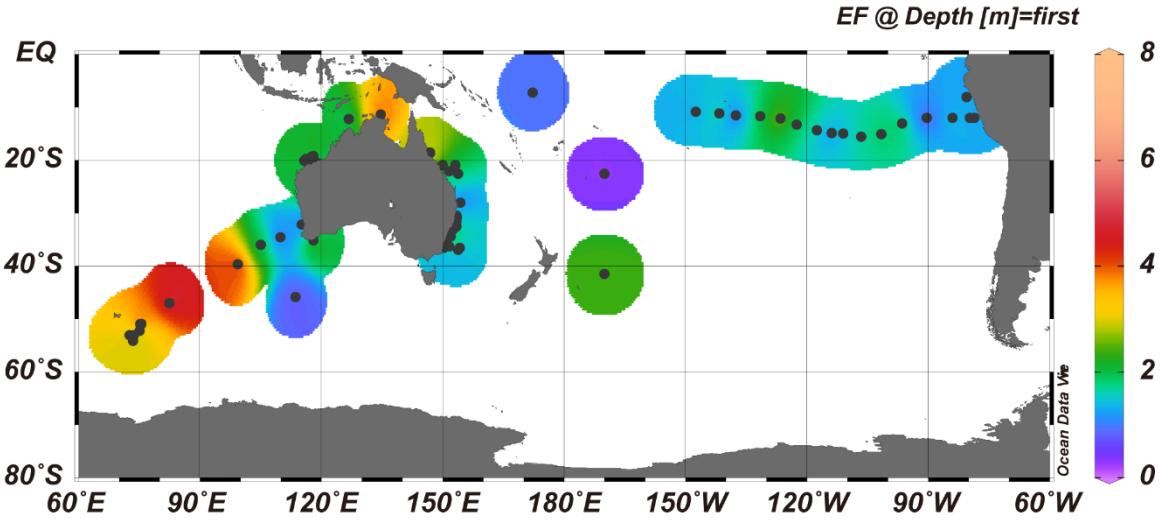


**Figure S6.** Spatial distribution of EFs in South Pacific TSP. The figure was described using Ocean Data View (Schlitzer, 2025).

**Reference**

Sakata, K., Kurisu, M., Takeichi, Y., Sakaguchi, A., Tanimoto, H., Tamenori, Y. et al. (2022). Iron (Fe) speciation in size-fractionated aerosol particles in the Pacific Ocean: The role of organic complexation of Fe with humic-like substances in controlling Fe solubility, Atmospheric Chemistry Physics, 22, 9461–9482, https://doi.org/10.5194/acp-22-9461-2022.

Sakata, K., Kurisu, M., Tanimoto, H., Sakaguchi, A., Uematsu, M., Miyamoto, C., Takahashi, Y. (2018) Custom-made PTFE filters for ultra-clean size-fractionated aerosol sampling for trace metals. Marine Chemistry, 206, 100– 108. https://doi.org/10.1016/j.marchem.2018.09.009.

Schlitzer, R.: Ocean Data View, https://odv.awi.de (last access: 19 September 2026), 2025.